Kinetic EPR studies of the addition of carbohydrate-derived radicals to methacrylic acid

Bruce C. Gilbert,*[a] John R. Lindsay Smith,[a] Steven R. Ward,[a] Adrian C. Whitwood[a] and Philip Taylor[b]

[a] *Department of Chemistry, University of York, Heslington, York, UK YO1 5DD*
[b] *Research Department, ICI Paints plc, Wexham Road, Slough, UK SL2 5DS*

EPR spectroscopy has been employed directly to monitor the initial stages in the free-radical copolymerisation of carbohydrates and methacrylic acid, initiated by a metal–peroxide couple. For the addition of a variety of oxygen-conjugated substrate-derived radicals (including those from *myo*-inositol, α- and β-D-glucose, D-fructose and sucrose) the rate constants are in the range (0.3–3.8) × 10^6 dm^3 mol^{-1} s^{-1}; in contrast $^{\bullet}CH_2OH$ has a value of 6 × 10^6 and α,α-dioxygen-substituted radicals have values of *ca.* 10^7 dm^3 mol^{-1} s^{-1}.

The reaction is clearly assisted by the +M electronic effect of the α-oxygen and by bending at the radical centre (for α-dioxygen-substituted species). The reaction rate is, however, reduced by β-oxygen substituents, especially through a SOMO–σ* (β-C–O) interaction, giving a substantial stereoelectronic retardation for axial β-oxygen substituents and for acyclic β-OH groups where eclipsing geometry (with respect to the radical centre) is favoured.

Introduction

Rate constants for the addition of a variety of small aliphatic radicals to acrylic acid and some simple derivatives in aqueous solution at room temperature have previously been found to be in the range 10^4–10^8 dm^3 mol^{-1} s^{-1}.[1–4] It has also been established, using a steady-state EPR method, that the reactions appear to be dominated by polar effects with, for acrylic acid itself, the order of reactivity $^{\bullet}Me < {}^{\bullet}CH_2OH < {}^{\bullet}CHMeOH$, with a notable increase in rate as the attacking radical becomes more nucleophilic.[4]

In the research to be described here, we set out to determine the rate constants, and their dependence on radical structure, for the reaction of a variety of carbohydrate-derived free radicals (and those from some further model compounds) with methacrylic acid; this is of particular relevance to understanding the behaviour of mixed carbohydrate–monomer systems in the presence of radical initiators (systems currently being explored as potential water-soluble copolymers). In particular we aimed to investigate the sensitivity of the rate constant to different substitution patterns, most notably to include steric effects, and the effect of β-substituents (steric and/or stereoelectronic), as revealed by changes in ring size and shape.

Results and discussion

Methodology

We have generally employed the Ti^{III}–H_2O_2 redox couple together with a rapid-flow continuous mixing system in the cavity of an EPR spectrometer. The experimental basis has been described previously: reaction (1) leads to the formation of hydroxyl radicals whose reaction in the cavity with an excess of added substrate [reaction (2)] normally leads to the detection of the radical(s) $R^{\bullet}$, the identity of which can be confirmed and steady-state concentration determined. As we have previously shown,[4] kinetic information can be obtained by application of steady-state analysis, which for a simple system [reactions (1)–(3)] gives eqn. (4)[5] (where subscript t refers to the concentrations in the cavity).

$$Ti^{III} + H_2O_2 \longrightarrow Ti^{IV} + HO^{\bullet} + HO^{-} \quad (1)$$

$$HO^{\bullet} + RH \longrightarrow H_2O + R^{\bullet} \quad (2)$$

$$R^{\bullet} + R^{\bullet} \longrightarrow \text{Non-radical products} \quad (3)$$

$$k_1[Ti^{III}]_t[H_2O_2]_t = 2k_3[R^{\bullet}]^2 \quad (4)$$

In initial experiments we utilised concentrations of reagents (after mixing) as follows, in a three-stream mixer at pH 4 (time between mixing and observation *ca.* 39 ms): $[Ti^{III}]$ 1.7 × 10^{-3} mol dm^{-3}, $[H_2O_2]$ 8.3 × 10^{-3} mol dm^{-3}, [substrate] = 0.1 mol dm^{-3}. Under these conditions, $^{\bullet}OH$ should be scavenged so that the steady state eqn. (4) applies. Examples which illustrate the types of results obtained for carbohydrate and related systems are illustrated in Fig. 1, which shows the spectra obtained from *myo*-inositol [Fig. 1(a): with assignments to radicals **1**–**6**,

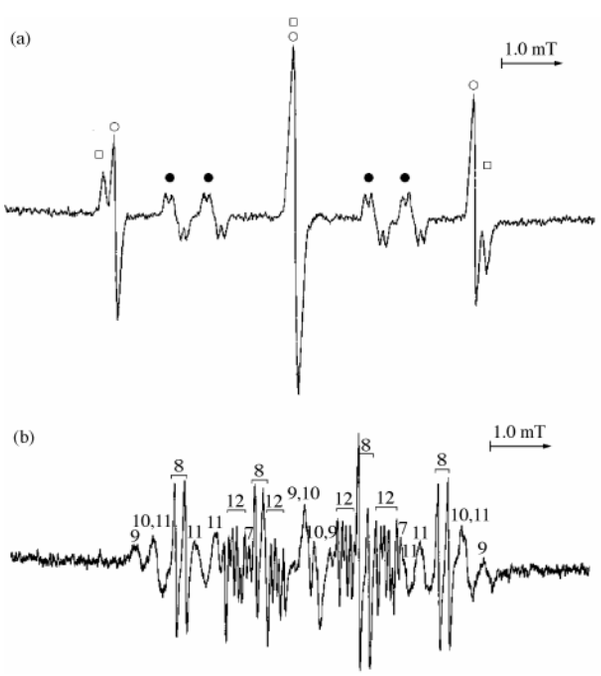

Fig. 1 (a) EPR spectra of radicals **1**–**6** obtained from the reaction of $^{\bullet}OH$ (from Ti^{III}–H_2O_2) and *myo*-inositol in aqueous solution at pH 4. For conditions see text. ○ = signals assigned to radicals **1** and **2**; □ = signals assigned to radicals **3** and **4**; ● = signals assigned to radicals **5** and **6**. (b) EPR spectra of the radicals **7**–**12** obtained from the reaction of $^{\bullet}OH$ (from Ti^{III}–H_2O_2) and α-D-glucose in aqueous solution at pH 4.

Table 1 EPR hyperfine splittings for carbohydrate-derived radicals and rate constants for their addition to methacrylic acid

Substrate	Radical structure	Hyperfine splittings[a]			$k_s/10^6$ dm^3 mol^{-1} s^{-1}
		a (α-H)	*a* (β-H)	*a* (Other)	
myo-Inositol					
1	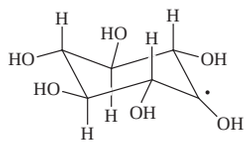		3.005 (2)	0.062 (2)	3.4 ± 0.25
2	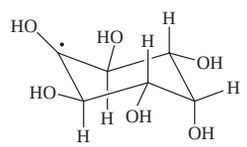		3.160 (2)	0.039 (2) 0.029 (1)	3.4 ± 0.25
3	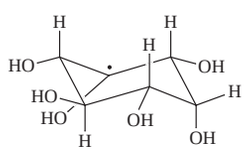		3.020 (1) 2.985 (1)	0.036 (1)	3.4 ± 0.25
4	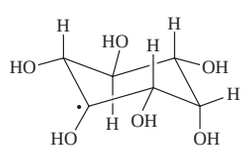		3.020 (1) 2.985 (1)	0.036 (1)	3.4 ± 0.25
5	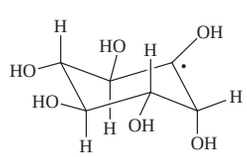		3.315 (1) 0.625 (1)	0.130 (1) 0.105 (1) 0.075 (1) 0.033 (1)	*b*
6	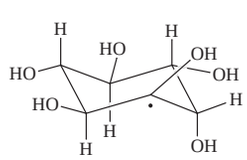		3.315 (1) 0.625 (1)	0.130 (1) 0.105 (1) 0.075 (1) 0.033 (1)	*b*
α-D-Glucose					
7	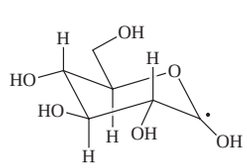		3.470 (1)	0.260 (5) 0.165 (1)	*b*
8	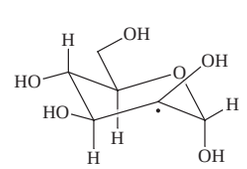		2.973 (1) 1.310 (1)	0.160 (1)	0.91 ± 0.15
9	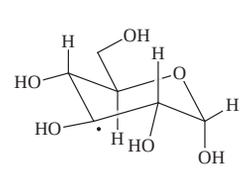		2.933 (1) 2.760 (1)		*b*
10	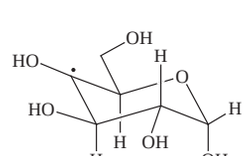		2.460 (1) 2.600 (1)	0.040 (1)	*b*

Table 1 (*Contd.*)

Substrate	Radical structure	Hyperfine splittings[a] *a* (α-H)	*a* (β-H)	*a* (Other)	$k_s/10^6$ dm^3 mol^{-1} s^{-1}
α-D-Glucose					
11	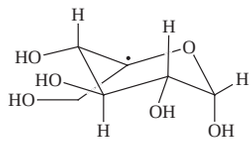		3.333 (1) 0.693 (1) 0.987 (1)		0.48 ± 0.06
12	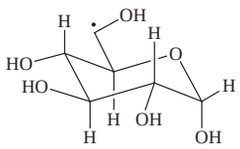	1.840 (1)	0.627 (1)	0.140 (1) 0.133 (1) 0.080 (1)	0.48 ± 0.05
β-D-Glucose					
13	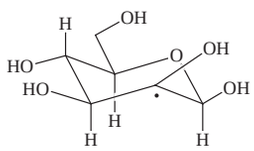		2.874(1) 2.280(1)		3.8 ± 0.5
D-Fructose					
14	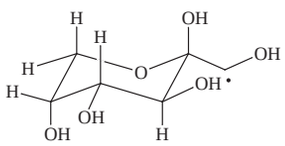		1.813 (1)	0.100 (1) 0.050 (1)	*b*
15	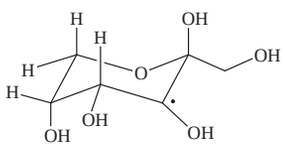		3.867 (2)	0.160 (1) 0.050 (1)	*b*
16	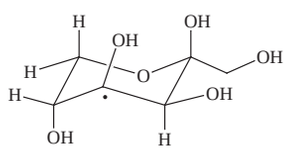		3.440 (1) 0.907 (1)		*b*
17	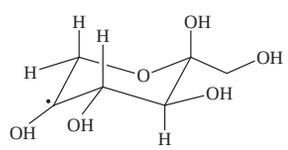		2.400 (1) 1.267 (1)		3.15 ± 0.26
18	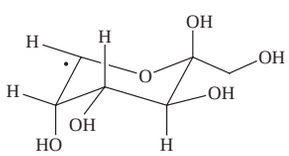	1.933 (1)	0.293 (1)		0.95 ± 0.07
19	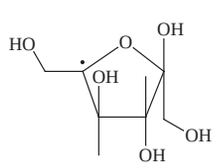		2.493 (1) 0.880 (2)		*b*
Sucrose					
20	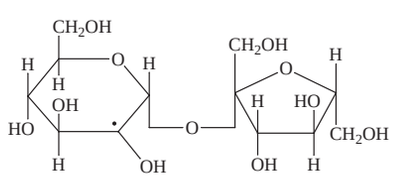		3.100 (1) 1.270 (1)	0.050 (2)	*b*

Table 1 (*Contd.*)

Substrate	Radical structure	Hyperfine splittings[a] *a* (α-H)	*a* (β-H)	*a* (Other)	$k_5/10^6$ dm^3 mol^{-1} s^{-1}
Sucrose					
21	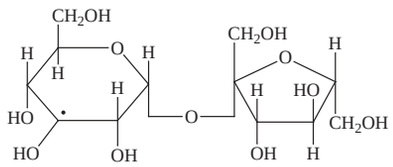		3.100 (1) 2.820 (1)	0.045 (2)	*b*
22	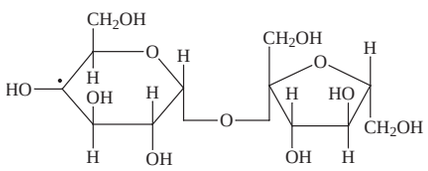		2.590 (1) 2.515 (1)		*b*
23	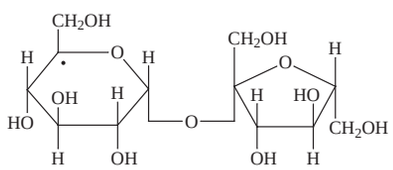		3.307 (1) 0.960 (1) 0.693 (1)		*ca*. 0.3
24	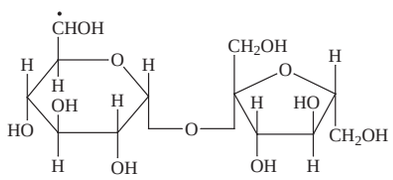	1.850 (1)	0.585 (1)	0.140 (1) 0.125 (1) 0.075 (1)	*b*
25	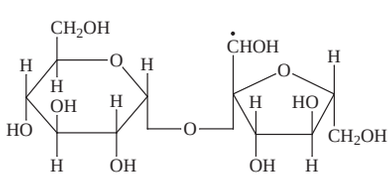	1.770 (1)			*b*
26	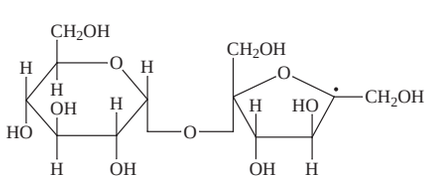		2.950 (1) 0.965 (1) 0.940 (1)	0.050 (2)	*ca*. 0.5

[a] mT, ±0.005 mT; all radicals $g = 2.0031 \pm 0.0005$. [b] Kinetic data could not be obtained for these radicals.

see Table 1] and α-D-glucose [Fig. 1(b): with assignments to radicals **7**–**12**].

The following points should be noted. Firstly there is excellent resolution in the multi-lined spectra, which allows carbon-centred radicals formed by attack of $^{\bullet}$OH at each position to be characterized (see Table 1). Secondly, the radicals can generally be characterized on the basis of hyperfine splittings assigned on the basis of conformational arguments described in detail earlier;[6,7] these will not be repeated here, except to emphasise that the β-axial and β-equatorial proton splittings (with the former much larger, typically in the range 2.6–3.5 mT) reflect the nature of the hyperconjugative ($B\cos^2\theta$ type) interaction between the unpaired electron and the β-C–H bonds.[8] Thirdly, the relative intensities of the individual signals reflect the relative reactivity of $^{\bullet}$OH at each position (which appears to be more or less statistical in most cases), on the assumption that all the radicals have approximately the same termination rate constant(s). Results for a range of carbohydrates and model substrates are described below.

Experiments were then carried out in which low concentrations of methacrylic acid, typically 0.001–0.005 mol dm^{-3}, were also present. At concentrations < 0.001 mol dm^{-3} no new signals could be detected; under these conditions there was no evidence for adducts formed from the reaction of either $^{\bullet}$OH or carbohydrate-derived radicals with the alkene. The latter is expected, given the much higher concentration of carbohydrate so that it scavenges $^{\bullet}$OH (k for the reaction of $^{\bullet}$OH and monosaccharide is expected to be *ca*. 1.5×10^9 dm^3 mol^{-1} s^{-1}; k for the reaction of $^{\bullet}$OH and methacrylic acid is 2.9×10^9 dm^3 mol^{-1} s^{-1}).[9,10] However, as the concentration of monomer was increased the carbohydrate-derived signals were found to be steadily reduced in intensity and new signals could be detected for radicals assigned to the adducts between carbohydrate-derived species, R$^{\bullet}$, and the alkene [reaction (5)]. For example,

$$R^{\bullet} + CH_2{=}CMeCO_2H \longrightarrow RCH_2\dot{C}MeCO_2H \quad (5)$$

Fig. 2 shows the spectra of radicals derived from *myo*-inositol and methacrylic acid; at concentrations of the latter in the range 0.001–0.01 mol dm^{-3} the decrease in intensity of the signals due to radicals **1**–**4** can be clearly seen. Signals from **5** and **6** are also lowered but as the concentration of the alkene is

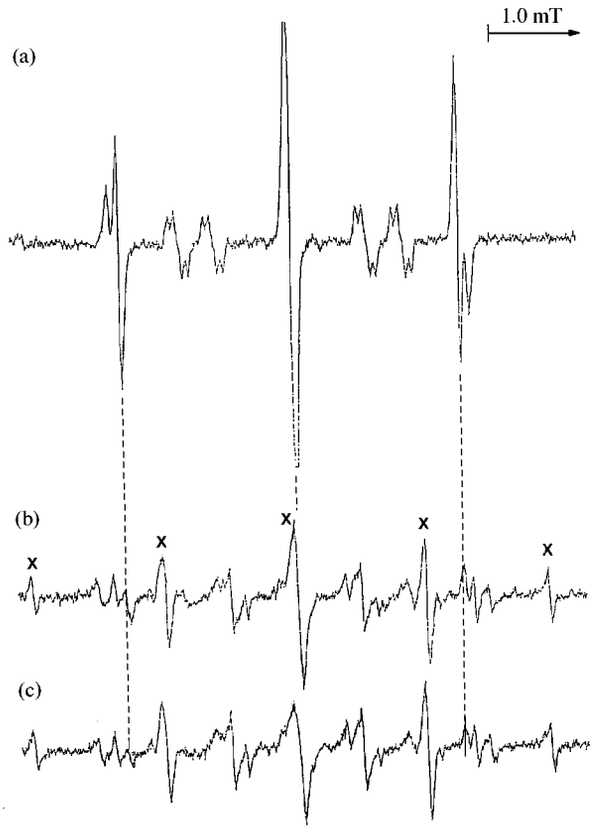

Fig. 2 EPR spectra from the reaction of $^{\bullet}OH$ (Ti^{III}–H_2O_2) with excess *myo*-inositol (0.1 mol dm^{-3}) showing the effect of addition of methacrylic acid [(a) absent, (b) 0.005 mol dm^{-3}, (c) 0.010 mol dm^{-3}]. The decay of the signals due to radicals **1** and **2** is indicated by a dotted line. × = signals assigned to *myo*-inositol–methacrylic acid adduct radicals.

increased the new adduct signals partially obscure these signals making it impossible to obtain quantitative data. At higher concentrations of alkene, additional signals from the $HO^{\bullet}$ adduct to the alkene can be detected, with splittings as previously noted [reaction (6)].

$$HO^{\bullet} + CH_2{=}CMeCO_2H \longrightarrow HOCH_2\dot{C}MeCO_2H \quad (6)$$

We have studied in detail the decrease in initial radical concentration as small amounts of alkene are added, conditions under which we believe the reactions involved to be (1), (2) and (5), as well as radical termination (the full analysis is given below). We have been able in this way to follow the very different 'decay' profiles (reduction in radical intensities) of individual radicals obtained initially from a given substrate.

For example, Fig. 3 shows the reduction in the steady-state concentration of *myo*-inositol-derived radicals **1**–**4** as the concentration of methacrylic acid is increased; it is also replotted to show the variation of $([R^{\bullet}_i]_0/[R^{\bullet}_i])-1$, where $[R^{\bullet}_i]$ refers to the concentration of a specific radical from a substrate RH and $[R^{\bullet}_i]_0$ is the concentration of that radical which is observed in the absence of methacrylic acid, a relationship which, as we shall show later, is expected to be linear. Fig. 4 illustrates the related plot for the C_2- and C_6-derived radicals from α-D-glucose (**8** and **12**, respectively), which are the best defined in the spectra. Other radical signals also decrease but the spectral complexity does not allow detailed quantitative information to be obtained. It is clear that the rate constant for addition of the different radical types is strongly dependent upon structure; and that the rate constants for addition to methacrylic acid are in the order: *myo*-inositol radicals **1**–**4** > α-D-2-glucosyl radical **8** > α-D-6-glucosyl radical **12**.

Kinetic approach

We have, as before,[4] assumed that a steady state exists in the

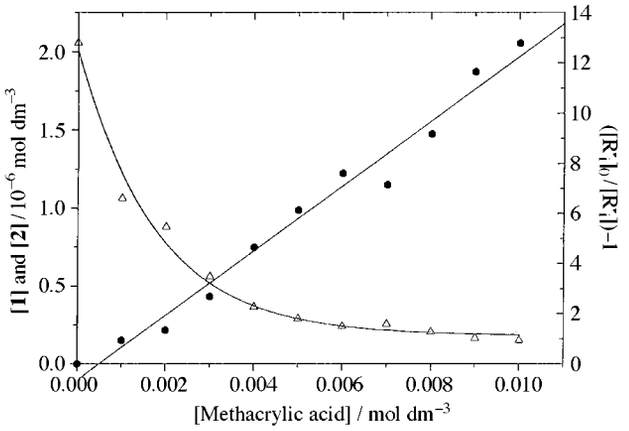

Fig. 3 Variation in the steady-state concentration of the radicals from *myo*-inositol (△) **1** and **2** as [methacrylic acid] is increased (see Fig. 2), together with the variation of $([R^{\bullet}_i]_0/[R^{\bullet}_i]-1)$ R = **1** and **2** (●)

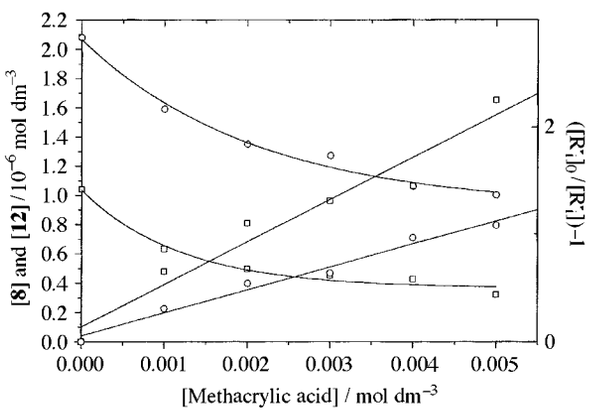

Fig. 4 Variation in the steady-state concentration of the radicals from α-D-glucose (□) and (○), **8** and **12** respectively, as [methacrylic acid] is increased together with the variation of $([R^{\bullet}_i]_0/[R^{\bullet}_i]-1)$

spectrometer cavity and that the necessary reactions for inclusion are those between Ti^{III} and H_2O_2 [reaction (1)], $HO^{\bullet}$ + RH [reaction (2)], $R^{\bullet}$ and alkene, to give a new radical $A^{\bullet}$ [eqn. (5)] and termination reactions between $R^{\bullet}$ and $R^{\bullet}$, $A^{\bullet}$ and $A^{\bullet}$ and $R^{\bullet}$ and $A^{\bullet}$. At zero alkene concentration, $[R^{\bullet}_i] = [R^{\bullet}_i]_0$, and steady-state analysis leads to eqns. (7) and (8) (in which $R^{\bullet}_i$

$$\frac{d[R^{\bullet}_i]}{dt} = k_2[HO^{\bullet}][RH] - 2k_3[R^{\bullet}_i]_0[R^{\bullet}]_T = 0 \quad (7)$$

$$k_2[HO^{\bullet}][RH] = 2k_3[R^{\bullet}_i]_0[R^{\bullet}]_T \quad (8)$$

refers to a specific radical from a substrate RH, the total radical concentration being $[R^{\bullet}]_T$). When an alkene is also present, at relatively low concentrations (so that the reaction of alkene with $^{\bullet}OH$ can be ignored), steady-state analysis leads to eqns. (9) and (10); we have assumed that all the termination reactions

$$\frac{d[R^{\bullet}_i]}{dt} = k_2[HO^{\bullet}][RH] - 2k_3[R^{\bullet}_i][R^{\bullet}]_T - k_5[\text{alkene}][R^{\bullet}_i] = 0 \quad (9)$$

$$= 2k_3[R^{\bullet}_i]_0[R^{\bullet}]_T - 2k_3[R^{\bullet}_i][R^{\bullet}]_T - k_5[\text{alkene}][R^{\bullet}_i] \quad (10)$$

have the same rate constant, k_3, for a given system (of the order 10^9 dm^3 mol^{-1} s^{-1}, see later). This leads to eqn. (11) and hence

$$\frac{k_5[\text{alkene}]}{2k_3[R^{\bullet}]_T} = \frac{[R^{\bullet}_i]_0 - [R^{\bullet}_i]}{[R^{\bullet}_i]} \quad (11)$$

(12) which should describe the behaviour of $[R^{\bullet}_i]$ as $[\text{alkene}]_i$ is

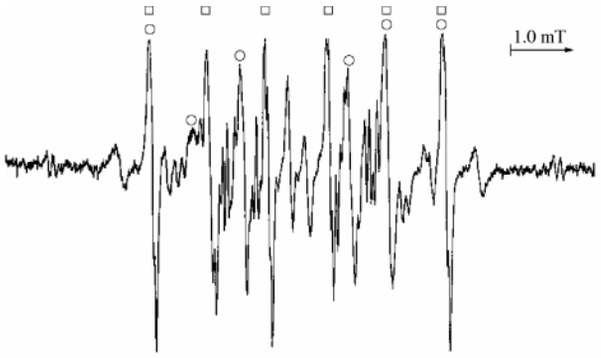

Fig. 5 EPR spectra of radicals **20**–**26** obtained from the reaction of $^{\bullet}OH$ (from Ti^{III}–H_2O_2) and sucrose in aqueous solution at pH 4. ○ = signals assigned to radical **23**; □ = signals assigned to radical **26**.

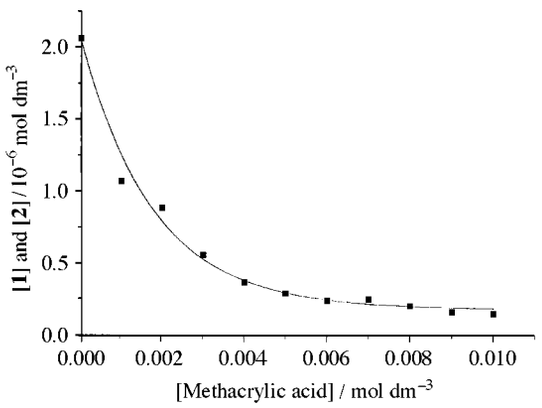

Fig. 6 Comparison of computer-simulated data (——) with experimental results (■) for the decay of the concentration of *myo*-inositol radicals **1** and **2** against concentration of methacrylic acid

$$\frac{k_5[\text{alkene}]}{2k_3[R^{\bullet}]_T} = ([R^{\bullet}_i]_0/[R^{\bullet}_i]) - 1 \qquad (12)$$

varied. Since $2k_3[R^{\bullet}]_T$ is considered to be constant (given that $[R^{\bullet}_i]$ is independent of the concentration of alkene if we make the assumption that the rate constants for all radical–radical reactions are the same in a given reaction system) it follows that the relationship should be linear.

We have analysed our results according to eqn. (12) for *myo*-inositol and for those systems where individual radicals (and their decrease) can be clearly followed; as shown in Figs. 3 and 4, the predicted behaviour is indeed observed within experimental error.

In order to estimate k_5 from the plots, we have used values of $2k_3[R^{\bullet}]_T$ obtained by comparison, *via* double integration of the spectra, with that obtained under identical conditions from $^{\bullet}CH_2OH$, derived from the reaction of methanol with $HO^{\bullet}$, for which the values of $2k_3$ and $[R^{\bullet}]_T$ are known (the value of $2k_3$ is given in ref. 11). By comparison of the areas of the integrated spectra the value of $[R^{\bullet}]_T$ for the carbohydrate-derived radicals can be calculated; given that $2k_3[R^{\bullet}]_T^2$ is constant then this value can be used to determine $2k_3$ for the carbohydrate-derived radicals. This approach leads to values of $2k_3$ of $(0.4 \pm 0.05) \times 10^9$ dm^3 mol^{-1} s^{-1} for *myo*-inositol, $(0.3 \pm 0.05) \times 10^9$ dm^3 mol^{-1} s^{-1} for monosaccharide-derived radicals and $(0.09 \pm 0.005) \times 10^9$ dm^3 mol^{-1} s^{-1} for radicals derived from the disaccharide sucrose (see later).

Analysis has been carried out for a variety of sugar-derived radicals **1**–**26**, obtained from *myo*-inositol, α- and β-D-glucose, sucrose and D-fructose (the latter studied after the solution of the substrate had been allowed to mutarotate to equilibrium, 70% β-D-fructopyranose and 23% β-D-fructofuranose). The EPR parameters are listed in Table 1 and are in close agreement with those reported previously,[6,7,12–14] although in the case of sucrose, distinction can now be made between the dominant C-5-derived radical in the five-membered ring **26** and the C-5-derived radical in the six-membered ring **23** (Fig. 5). Kinetic analysis according to eqn. (12) leads to the rate constants for addition to methacrylic acid shown in Table 1; the values are believed to be accurate to within ±15%, except in cases where signal overlay makes the measurement more difficult, *e.g.* **9**–**11**.

We have also verified our analysis of the observed behaviour of the *myo*-inositol radicals **1** and **2** by the use of a kinetic simulation program (Fig. 6), in which parameters are entered for the rates of reaction of the hydroxyl radical with the carbohydrate, the hydroxyl radical reaction with the alkene, the addition reaction of the carbohydrate-derived radical with the alkene (obtained experimentally) and values for $2k_3$ (as above). Given the relative concentrations of carbohydrate and alkene the program produces a plot of radical concentration against alkene concentration which can be compared with the experimental data and in this case and others gives an excellent fit, as illustrated in Fig. 6.

The results in Table 1 show that the rate constants of the monosaccharide-derived radicals vary from the value of *ca.* 3.5×10^6 dm^3 mol^{-1} s^{-1} for the *myo*-inositol radical(s) **1**–**4** and the β-D-2-glucosyl radical **13** through the value of 0.91×10^6 dm^3 mol^{-1} s^{-1} for the isomeric α-D-2-glucosyl radical **8** down to 0.48×10^6 dm^3 mol^{-1} s^{-1} for the α-D-6-glucosyl radical **12** (*i.e.* by a factor of *ca.* 8 overall). For the disaccharide sucrose we note the relatively slow reactions of the corresponding C-5 species from the six- and five-membered rings, k(**23**) = 0.3×10^6 dm^3 mol^{-1} s^{-1} and k(**26**) = 0.5×10^6 dm^3 mol^{-1} s^{-1}, respectively. In comparison, the rate constant for attack of $^{\bullet}CHMeOH$ on methacrylic acid is *ca.* 10^7 dm^3 mol^{-1} s^{-1}.[4]

One possible explanation which may contribute to the main trend observed is the presence of a significant steric or stereoelectronic effect whose origin may well reflect the presence and orientation of the C–O bonds in the β-position with respect to the radical centre. It may be particularly relevant that, as we have noted before in comparing the structural properties of, *e.g.* $^{\bullet}CH_2OH$ and $^{\bullet}CH(OH)CH_2OH$, radicals of the latter type exhibit a strong interaction between the radical centre on the α-carbon and the β-C–O bond [reflecting the juxtaposition of α-(+M) and β-(−I) substituents] which leads to a locked (eclipsed) conformation (see **27**) and flattening at α-carbon [an effect which is revealed in the EPR spectrum by, for example, the very low value of a(β-H)].[15] This can be interpreted in terms of the overlap between SOMO and β-C–O σ* orbitals (maximised in **27**),[16] or in valence bond terms by the contribution of structures as **28**–**30**:

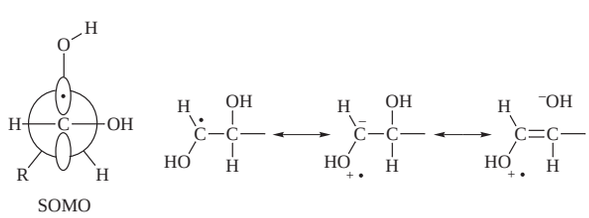

27 **28** **29** **30**

Kinetic study model compounds

A range of simple model substrates was thus next chosen, so as to be able to explore the separate effects of a β-OH group (in locked conformation), the roles of α- and/or β-OR groups (radicals **31**–**34**), as well as the addition of some α-dioxygen-substituted radicals which have considerable distortion from planarity and, presumably, enhanced electron density at C-α and hence nucleophilicity (radicals **35** and **36**): the (bent) structure of the 1,3-dioxolan-2-yl (**35**) and 1,3,5-trioxolan-2-yl radicals (**36**) is firmly established.[17,18] Hyperfine splitting

Table 2 Rate constants for the addition of radicals formed from model compounds to methacrylic acid

Substrate	Radical		$k_5/10^6$ dm^3 mol^{-1} s^{-1}
Ethane-1,2-diol	$^{\bullet}CH(OH)CH_2OH$	**31**	1.1 ± 0.1
2-Methoxyethanol	$^{\bullet}CH(OH)CH_2OMe$	**32**	1.7 ± 0.3
	$^{\bullet}CH(OMe)CH_2OH$	**33**	2.2 ± 0.2
1,3-Dioxolane		**34**	*ca*. 10
		**35**	*ca*. 25
1,3,5-Trioxane		**36**	*ca*. 10

constants of the radicals **31**–**36** have been previously reported and will not be reported here.[17,18]

In each case the experimental data were analysed by eqn. (12) and linear plots (*cf*. Figs. 3 and 4) were obtained. The values of k_5 calculated from these plots were confirmed by computer simulation. The results obtained are summarised in Table 2.

Interpretation of results

Comparison of the kinetic results in Tables 1 and 2 with the findings for $^{\bullet}CHMeOH$ and $^{\bullet}CH_2OH$ (rate constants for addition to methacrylic acid 10^7 and 6×10^6 dm^3 mol^{-1} s^{-1}, respectively)[4] immediately allows several conclusions to be drawn about the rates of addition of oxygen-conjugated radicals to methacrylic acid.

(i) The presence of a β-oxygen substituent retards the addition, as would be expected on the basis of its −I effect; the attacking radical is now presumably less nucleophilic as the +M effect of the α-substituent is significantly reduced.

(ii) This retarding effect is particularly marked when the β-oxygen is placed in an eclipsing or axial position, allowing maximum SOMO–C–O σ* overlap [*cf*. $^{\bullet}CH(OH)CH_2OH$ (**31**) $k_5 = 1.1 \times 10^6$ dm^3 mol^{-1} s^{-1}, α-D-2-glucosyl radical (**8**) $k_5 = 0.91 \times 10^6$ dm^3 mol^{-1} s^{-1}]; in contrast the rate constants for β-D-2-glucosyl (**13**) and the *myo*-inositol radicals **1**–**4**, with equatorial OHs, are greater than 3×10^6 dm^3 mol^{-1} s^{-1}. The result for the α-D-6-glucosyl radical **12**, which has a particularly low value of k_5 0.48×10^6 dm^3 mol^{-1} s^{-1}, presumably arises from the eclipsing nature of the β-O–R bond, reflected in the particularly low β-proton hyperfine splitting of 0.627 mT (**37**).

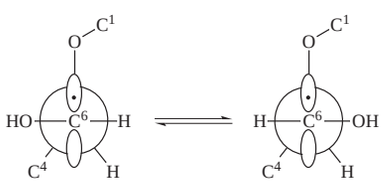

37

It is also worth noting that the α-D-2-glucosyl radical **8** reacts slightly faster than the α-D-6-glucosyl radical **12**, as in the latter the SOMO is perfectly eclipsed with the β-C–O bond whereas in the case of the α-D-2-glucosyl radical **8** an angle of approximately 30° exists between the SOMO and the axial β-C–O bond. Hence radical **8** is not as stabilised as radical **12** and therefore it is more nucleophilic.

It is also very notable that there is no reduction of the rate constant of **34** ($k_5 = 10 \times 10^6$ dm^3 mol^{-1} s^{-1}) for which the β-C–O bond is orthogonal to the SOMO.

(iii) Similar effects are observed for the sucrose-derived radicals **23** and **26**. It is of particular note that the radical derived from the five-membered ring (**26**) has a higher value of k_5 than the equivalent radical from the six-membered ring (**23**), although both are observed to react slower than the monosaccharide radicals due to increased bulk. This is believed to reflect the better overlap of the SOMO with the lone pair orbital of the ring oxygen in a more nearly planar five-membered ring than is possible in a six-membered ring (*cf*. radical **34**). The preponderance of radical **26** is also notable (see Fig. 5), as observed before overlap of this lone pair orbital with the C–H bond at the C-5 position evidently weakens the bond, making it more prone to abstraction by the hydroxyl radical, hence the signals due to radical **26** dominate the sucrose–HO$^{\bullet}$ EPR spectrum (Fig. 5).[14]

(iv) As judged by the rate constants for $^{\bullet}CH(OH)CH_2OMe$ (**32**) and $^{\bullet}CH(OMe)CH_2OH$ (**33**), the effects of α- and β-methoxy groups appear to parallel those of hydroxy substituents.

(v) The effect of a second α-oxygen substituent, which induces radical-centre bending on radicals such as **35** and **36**, evidently accelerates the rate of addition to methacrylic acid. This is presumably due to one or both of two effects. The first is the interaction between the SOMO and a lone pair from each α-oxygen atom, a phenomenon which in turn raises the energy of the orbital making the radical more nucleophilic (hence giving a high value of k_5). The second is due to the well-established pyramidal nature of the radical centre in these species (reflected in the EPR hyperfine splitting constants of radicals **35** and **36**).[17,18] It has been proposed that,[19] during radical addition reactions of this type, the attacking radical adopts a pyramidal conformation in the transition state. Given that this is an early transition state and the species involved are more reactant-like than product-like,[20] then the greater the extent of pyramidalisation in the radical centre, the lower the activation energy for the reaction.

Experimental

EPR spectra were recorded on a Bruker ESP 300 spectrometer equipped with an X-band microwave bridge and 100 kHz modulation. Hyperfine splittings and *g* values were determined directly from the spectrometer's field scan, this having been calibrated with the signal from Fremy's salt ($a_N = 1.3091$ mT,[21] *g* 2.0055[22]): data recorded in Table 1 were obtained under conditions of high resolution (low modulation amplitude). Radical concentrations were determined, *via* double integration, by comparison with the spectrum obtained from the $^{\bullet}CH_2OH$ radical, formed *via* the reaction of Ti^{III} and H_2O_2 in the presence of methanol. A mixing chamber was employed which allowed simultaneous mixing of three reagent streams *ca*. 30 ms before passage through the cavity of the spectrometer; flow was maintained using a Watson-Marlow 502S peristaltic pump placed on the inlet tubing. pH measurements were made using a Pye-Unicam PW9410 pH meter with the electrode inserted into the effluent stream. The three solutions typically contained (i) titanium(III) chloride (0.005 mol dm^{-3}) and EDTA (0.005 mol dm^{-3}), (ii) hydrogen peroxide (0.025 mol dm^{-3}) and (iii) the substrate (0.3 mol dm^{-3}) and methacrylic acid (0.0005–0.01 mol dm^{-3}); pH was adjusted to *ca*. 4 by addition of sulfuric acid (18 mol dm^{-3}) or ammonia solution (15 mol dm^{-3}) to the first stream and all solutions were deoxygenated by nitrogen purge both before and during use.

The kinetic simulation program was originally written by Dr T. M. F. Salmon and modified to run on an IBM-PC 486DX clone.

All chemicals employed were commercial samples used as supplied.

Acknowledgements

We thank the BBSRC and ICI Paints plc for a CASE award (to S. R. W.).

References

1 H. Fischer, *Adv. Polym. Sci.*, 1968, **5**, 463.
2 K. Münger and H. Fischer, *Int. J. Chem. Kinet.*, 1985, **17**, 809.
3 K. Héberger and H. Fischer, *Int. J. Chem. Kinet.*, 1993, **25**, 913.
4 B. C. Gilbert, J. R. Lindsay Smith, E. C. Milne, A. C. Whitwood and P. Taylor, *J. Chem. Soc.*, *Perkin Trans. 2*, 1993, 2025.
5 B. C. Gilbert, R. O. C. Norman and R. C. Sealy, *J. Chem. Soc.*, *Perkin Trans. 2*, 1973, 2174.
6 B. C. Gilbert, D. M. King and C. B. Thomas, *J. Chem. Soc.*, *Perkin Trans. 2*, 1980, 1821.
7 B. C. Gilbert, D. M. King and C. B. Thomas, *J. Chem. Soc.*, *Perkin Trans. 2*, 1981, 1186.
8 R. O. C. Norman and B. C. Gilbert, *Adv. Phys. Org. Chem.*, 1967, **5**, 53.
9 N. Motohashi and Y. Saito, *Chem. Pharm. Bull.*, 1993, **41**, 1842.
10 (*a*) G. V. Buxton, C. L. Greenstock, W. P. Helman and A. B. Ross, *J. Phys. Chem. Ref. Data*, 1988, **17**, 513; (*b*) Farhataziz and A. B. Ross, *Selected Specific Rates of Reactions of Transients from H_2O in Aqueous Solution III. Hydroxyl Radical and Perhydroxyl Radicals and their Radical Ions*, National Bureau of Standards, Washington, 1977; (*c*) A. Revvers, C. Greenstock, J. Borsa and J. Chapman, *Int. J. Radiat. Biol. Relat. Stud. Phys. Chem. Med.*, 1973, **24**, 533.
11 P. Neta, *Adv. Phys. Org. Chem.*, 1976, **12**, 223.
12 M. Fitchett, B. C. Gilbert and M. Jeff, *Philos. Trans. R. Soc. London*, *Ser. B*, 1985, **311**, 517.
13 M. Fitchett, B. C. Gilbert and R. L. Wilson, *J. Chem. Soc.*, *Perkin Trans. 2*, 1988, 673.
14 B. C. Gilbert, D. M. King and C. B. Thomas, *J. Chem. Soc.*, *Perkin Trans. 2*, 1983, 675.
15 A. J. Dobbs, B. C. Gilbert and R. O. C. Norman, *J. Chem. Soc.*, *Perkin Trans. 2*, 1972, 786.
16 I. Fleming, *Frontier Orbitals and Organic Reactions*, Wiley, New York, 1978.
17 A. J. Dobbs, B. C. Gilbert and R. O. C. Norman, *J. Chem. Soc. A*, 1971, 124.
18 C. Gaze and B. C. Gilbert, *J. Chem. Soc.*, *Perkin Trans. 2*, 1977, 754.
19 (*a*) R. Arnaud, R. Subra, V. Barone, F. Leilj, S. Olivella, A. Solé and N. Russo, *J. Chem. Soc.*, *Perkin Trans. 2*, 1986, 1517; (*b*) K. N. Houk, M. N. Paddon-Row, D. C. Spellmeyer, N. G. Rondan and S. Nagase, *J. Org. Chem.*, 1986, **51**, 2874; (*c*) T. Fueno and M. Kamanchi, *Macromolecules*, 1988, **21**, 908; (*d*) C. Gonzales, C. Sosa and H. B. Schlegel, *J. Phys. Chem.*, 1989, **93**, 2435; (*e*) M. Zipse, J. He, K. N. Houk and B. Giese, *J. Am. Chem. Soc.*, 1991, **113**, 4324.
20 K. Héberger, M. Walbiner and H. Fischer, *Angew. Chem.*, *Int. Ed. Engl.*, 1992, **31**, 635.
21 R. J. Faber and G. K. Fraenkel, *J. Chem. Phys.*, 1967, **47**, 2462.
22 J. Q. Adams, S. W. Nicksic and J. R. Thomas, *J. Chem. Phys.*, 1966, **45**, 654.

Paper 8/02390E
Received 27*th March* 1998
Accepted 24*th April* 1998